International Journal of Nanomedicine

Dovepress
open access to scientific and medical research

Open Access Full Text Article

ORIGINAL RESEARCH

Hydrophilic/Hydrophobic Janus Nanofibers Containing Compound K for Cartilage Regeneration

Hyun Ho Shin[1,*], Junyoung Park[2,*], Yeo-Jin Kim[3], Donghyeon Kim[2], Eun-Jung Jin[2,4], Ji Hyun Ryu[1,3,4]

[1]Department of Chemical Engineering, Wonkwang, University, Iksan, Jeonbuk, 54538, Republic of Korea; [2]Department of Biological Sciences, College of Natural Sciences, Wonkwang University, Iksan, Jeonbuk, 54538, Republic of Korea; [3]Department of Carbon Convergence Engineering, Smart Convergence Materials Analysis Center, Wonkwang University, Iksan, Jeonbuk, 54538, Republic of Korea; [4]Integrated Omics Institute, Wonkwang University, Iksan, Jeonbuk, 54538, Republic of Korea

*These authors contributed equally to this work

Correspondence: Ji Hyun Ryu, Department of Carbon Convergence Engineering, Iksan, Jeonbuk, 54538, Republic of Korea, Email jhryu4816@wku.ac.kr; Eun-Jung Jin, Department of Biological Sciences, Wonkwang University, Iksan, Jeonbuk, 54538, Republic of Korea, Email jineunjung@wku.ac.kr

Introduction: Cartilage regeneration is a challenging issue due to poor regenerative properties of tissues. Electrospun nanofibers hold enormous potentials for treatments of cartilage defects. However, nanofibrous materials used for the treatment of cartilage defects often require physical and/or chemical modifications to promote the adhesion, proliferation, and differentiation of cells. Thus, it is highly desirable to improve their surface properties with functionality. We aim to design hydrophilic, adhesive, and compound K-loaded nanofibers for treatments of cartilage defects.

Methods: Hydrophilic and adhesive compound K-containing polycaprolactone nanofibers (CK/PCL NFs) were prepared by coatings of gallic acid-conjugated chitosan (CHI-GA). Therapeutic effects of CHI-GA/CK/PCL NFs were assessed by the expression level of genes involved in the cartilage matrix degradation, inflammatory response, and lipid accumulations in the chondrocytes. In addition, Cartilage damage was evaluated by safranin O staining and immunohistochemistry of interleukin-1β (IL-1β) using OA animal models. To explore the pathway associated with therapeutic effects of CHI-GA/CK/PCL NFs, cell adhesion, phalloidin staining, and the expression level of integrins and peroxisome proliferator-activated receptor (PPARs) were evaluated.

Results: CHI-GA-coated side of the PCL NFs showed hydrophilic and adhesive properties, whereas the unmodified opposite side remained hydrophobic. The expression levels of genes involved in the degradation of the cartilage matrix, inflammation, and lipogenesis were decreased in CHI-GA/CK/PCL NFs owing to the release of CK. In vivo implantation of CHI-GA/CK/PCL NFs into the cartilage reduced cartilage degradation induced by destabilization of the medial meniscus (DMM) surgery. Furthermore, the accumulation of lipid deposition and expression levels of IL-1β was reduced through the upregulation of PPAR.

Conclusion: CHI-GA/CK/PCL NFs were effective in the treatments of cartilage defects by inhibiting the expression levels of genes involved in cartilage degradation, inflammation, and lipogenesis as well as reducing lipid accumulation and the expression level of IL-1β via increasing PPAR.

Keywords: polycaprolactone nanofibers, gallic acid-conjugated chitosan, compound K, hydrophilic coating, adhesive material, cartilage regeneration

Introduction

The treatment of articular cartilage defects, including osteoarthritis (OA), remains a major challenge owing to its inherently limited capacity for self-healing, primarily due to the absence of blood vessels and nerves.[1–5] To address this, researchers have focused on cartilage tissue engineering with particular attention to nanofibrous materials that may offer several advantages, such as the promotion of cell adhesion, proliferation, and differentiation, and the delivery of therapeutic drugs to treat cartilage defects.[6–11] In addition, the three-dimensional

Received: 12 August 2023
Accepted: 20 December 2023
Published: 1 March 2024

Graphical Abstract

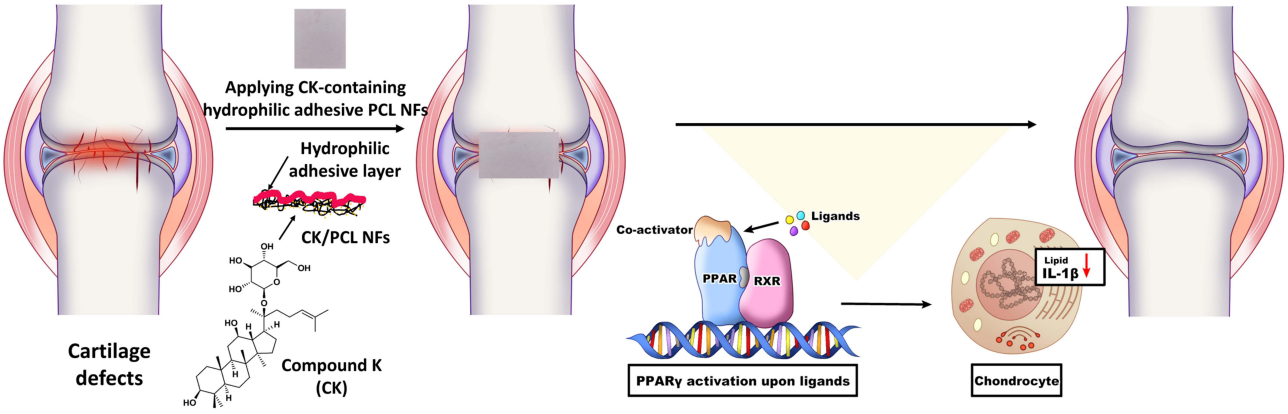

architecture of nanofibers can be readily obtained by electrospinning, self-assembly, and phase separation methods.[11–15] Furthermore, nanofiber modification stimulates chondrocyte growth and cartilage regeneration by providing a suitable microenvironment.[16–18] For instance, plasma-treated and cationized gelatin-immobilized poly (lactic acid) nanofibers showed tight attachment of chondrocytes with improved osteoblast proliferation and differentiation.[16] In addition, α-granules-encapsulated coaxial poly(ε-caprolactone)/poly(vinyl alcohol) nanofibers stimulate the viability and chondrogenic differentiation of mesenchymal stem cells.[17,18] Thus, the functionalization of nanofibrous materials is important for tailoring the physicochemical and biological properties of cartilage tissue engineering.

Polycaprolactone (PCL) is one of the most frequently used materials for the preparation of nanofibers by electrospinning. PCL-based nanofibers (PCL NFs) are promising materials for drug delivery depots and tissue engineering scaffolds because of their biocompatibility and biodegradability.[19–23] For instance, drug (ie, kaempferol-loaded albumin nanoparticles and dexamethasone)-encapsulated PCL NFs in human chondrocytes induce the deposition of glycosaminoglycans with a sustained release of drugs.[24] However, PCL-based nanofibers often require external agents for the tissue engineering because of their intrinsic surface properties of hydrophobic nature and poor interactions with biomolecules and cells.[25–29] To address this, co-electrospinning of hydrophilic polymers or physical/chemical modifications of PCL NFs can be used to increase hydrophilicity and bioactivity.[27,30–32] For instance, co-electrospun nanofibrous biomaterials and the immobilization of biomolecules (ie, poly(glycerol sebacate), gelatin-chondroitin sulfate, alginate, chondroitin sulfates, and hyaluronic acid) help improve the cartilage tissue engineering.[33–37] Co-electrospinning of PCL and gelatin-chondroitin sulfate enhances the attachments and proliferations of human bone mesenchymal stem cells (hMSC) with improved hydrophilicity.[34] In addition, hydrolysis and aminolysis of PCL NFs also reduce the water contact angles of NFs that can significantly enhance the cell attachments with increased cell viability.[27] Furthermore, the immobilization of carboxymethyl cellulose on the surface of PCL NFs enhances the osteochondral inductivity resulting in the induced osteochondral differentiations.[38]

Compound K (CK), a bioactive compound derived from ginsenosides, has been studied for its potential health benefits and physiological effects including anti-inflammatory, antioxidant, and anti-tumorigenic effects.[39–41] In osteoarthritis (OA) cartilage, up-regulated inflammatory mediators, ie, interleukin-1β (IL-1β), tumor necrosis factor-α (TNF-α), and interleukin-6 (IL-6) stimulated the production of reactive oxygen species (ROS) and the expression of matrix-degrading proteases that lead to the degradation of the cartilage matrix.[42] As the generation of ROS and inflammation are closely related to the development and progression of OA, CK may protect cartilage from degradation and promote its regeneration. Moreover, CK is known to inhibit matrix

metalloproteinases (MMPs), suggesting a chondroprotective role in the degradation of the cartilage matrix and preservation of structural integrity.[43] Although the potential application of CK in cartilage preservation and regeneration is promising, its efficacy and practical applications in cartilage regeneration need to be explored. Moreover, as the efficiency of CK delivery can be influenced by the specific characteristics of the cartilage tissue and joint OA environment, additional research may provide a deeper understanding of the most efficient way to deliver CK to the cartilage, as well as to protect CK from degradation, increase its stability, and prolong its residence time in the joint to optimize its regenerative effects.

Conjugation of phenolic compounds to polymeric backbones is a useful technique for the coating of biomaterials, as previously reported.[44–46] Along with the strong adhesiveness to tissue surfaces, the phenolic compounds have multiple functionalities with their bioactivities.[47–49] In this study, we introduce a facile method for preparing hydrophilic and adhesive drug-loaded PCL NFs using gallic acid-conjugated chitosan (CHI-GA). In addition, CK was used as a drug for the cartilage regenerations. The CHI-GA-coated CK/PCL NFs surfaces exhibited hydrophilic and cell/tissue adhesive properties that were responsible for the successful attachment of the CHI-GA/CK/PCL NFs to cartilage defects with the delivery of CK. In contrast, the unmodified side of the CK/PCL NFs remained hydrophobic. Implantation of CHI-GA/CK/PCL NFs into the destabilization of the medial meniscus (DMM) cartilage led to the inhibition of inflammation, lipid accumulation, and expression level of IL-1β resulting in the prevention of cartilage degradation.

Materials and Methods

Materials

Polycaprolactone (Mn. 80 kDa), chitosan (medium molecular weight, 200–800 cP), and gallic acid (GA) were purchased from Sigma-Aldrich (Milwaukee, WI, USA). N-hydroxysuccinimide (NHS) and 1-Ethyl-3-(3-dimethylaminopropyl) carbodiimide (EDC) were purchased from Tokyo Chemical Industry Co. Ltd. (TCI-SU, Tokyo, Japan). Ginsenoside Compound K (CK) from the roots of Panax ginseng C.A. Mey was purchased from ChemFaces (Wuhan, China). Chloroform and methyl alcohol were purchased from Samchun Pure Chemicals (Pyeongtaek, South Korea). All the other chemicals were of analytical grade.

Preparation of CK-Loaded PCL NFs (CK/PCL NFs)

CK-loaded PCL NFs were prepared by electrospinning. Briefly, PCL (9 wt%) was dissolved in a mixed solution of chloroform and methanol (3:1 v/v) and CK (9 mg) was added to the PCL solution. The final concentration of CK was 0.18 wt%. The CK/PCL solution was electrospun using 18-gauge needles at a voltage of 17 kV and a flow rate of 15 L/min using an electrospinning/spray system (ESR100D, NanoNC, Seoul, South Korea). The distance between the needle and the collector wrapped with aluminum foil was 18 cm.

Synthesis of Gallic Acid-Conjugated Chitosan (CHI-GA)

CHI-GA was synthesized using an EDC coupling agent, as previously reported.[50,51] Briefly, chitosan (500 mg) was dissolved in distilled deionized water (DDW, 44.5 mL) containing 5 mL of 1 N HCl. The pH was adjusted to 5 by adding 1 N NaOH. After the complete dissolution of chitosan, GA (467 mg), EDC (526 mg), and NHS (316 mg) in ethanol (25 mL) were added to the chitosan solution and allowed to react for 12 h. The pH of the solution was maintained at 4.5 to 5.5 during the reactions. The product was purified using a dialysis membrane (MWCO = 3.5 kDa, SpectraPor, Spectra Labs, Rancho Dominguez, CA, USA) against a NaCl solution (pH 2.0, 10 mM) for 2 d and DDW for 4 h and was lyophilized. The gallic acid conjugation of CHI-GA was confirmed using UV-Vis spectroscopy (UV-1900i, Shimadzu, Japan).

Preparation of CHI-GA-Coated CK/PCL NFs (CHI-GA/CK/PCL NFs)

To prepare the CHI-GA/CK/PCL NFs, CHI-GA was dissolved in PBS solution (pH 7.4) with a concentration of 2 mg/mL. After the complete dissolution of CHI-GA, the CK/PCL NFs were placed onto the CHI-GA solution and allowed to react for 8

h in incubators at 37 °C. During the reactions, the CK/PCL NFs floated on the CHI-GA solution owing to the hydrophobic properties of the PCL NFs. After incubation, the CHI-GA/CK/PCL NFs were vigorously washed with PBS and DDW, at least three times each. Due to the hydrophobicity of CK/PCL NFs, the CHI-GA was coated on one side of CK/PCL NFs. The final CHI-GA/CK/PCL NF products were freeze-dried and stored in a moisture-free desiccator until further use.

Morphological Analysis of CHI-GA/CK/PCL NFs

The morphology of the CHI-GA/CK/PCL NFs was analyzed using scanning electron microscopy (SEM, S-4800, Hitachi Ltd., Tokyo, Japan) at an acceleration voltage of 15 kV at the Core Facility for Supporting Analysis & Imaging of Biomedical Materials at Wonkwang University, which is supported by the National Research Facilities and Equipment Center. Briefly, PCL, CK/PCL, and CHI-GA/CK/PCL NFs (1 × 1 cm^2) were placed on SEM holders using carbon tapes. The NFs were coated with platinum before the SEM images were obtained.

For the morphological analysis after cell attachment tests, the iMAC cell suspension (20 μL of 5×105 cell/mL) was seeded onto nanofibers and incubated for 1 h at 37 °C. Loose and unadhered cells were removed. The wells were gently washed twice with PBS. The adherent cells were fixed with 4% paraformaldehyde in PBS for 15 min. Once the fixation was completed, the samples were dehydrated with ethanol at serially increasing concentrations of 25, 50, 75, 90, and 100%.

Study on Tissue Adhesive Properties

Tissue adhesiveness of the CHI-GA/CK/PCL NFs was examined using a universal testing machine (UTM, Instron 5583, Instron, USA) equipped with a 50 N load cell according to previous research with a slight modification.[50–52] The PCL sides of the CHI-GA/CK/PCL NFs (1 × 1 cm^2) were attached to the PET film (1 × 5 cm^2) using commercially available adhesives (Loctite® 401, Rocky Hill, Connecticut, USA) resulting in the exposure of the CHI-GA-coated surfaces. In addition, the porcine intestine (1 × 1 cm^2) was attached to a PET film (1 × 5 cm^2) using commercially available adhesives. After washing the CHI-GA/CK/PCL NFs and porcine intestine on the PET films, both were overlapped and pushed. The tensile strengths were measured by pulling the film at a loading rate of 1 mm/min. All measurements were performed in triplicate.

Immature Mouse Articular Chondrocyte (iMACs) Culture

The iMACs were isolated from postnatal day 5 pups and were cultured with Dulbecco's modified Eagle's medium (DMEM; Gibco) with 10% fetal bovine serum (FBS; Gibco) and 100 units/mL of penicillin and streptomycin at 37 °C supplied with 5% CO_2.

Immunocytochemistry

For actin staining, up to 10,000 cells were seeded on 12 mm coverslips coated with BSA, CHI, or CHI-GA. After 24 hr, the cells were fixed in 4% PFA for 20 min, permeabilized with Triton X-100 in PBS, incubated with 1% BSA in PBS for 1 h, stained with Alexa488-phalloidin (1: 500 dilution, Molecular Probes, Eugene, OR) for 1 h at RT and incubated with DAPI (1: 1000 dilution) solution in PBS.

Experimental Animals

Wild-type C57BL/6N mice were purchased from Samtako BioKorea, Inc. (Osan, Korea). All mice were housed at 22 ± 1°C with 12 h light/dark cycles and a relative humidity of 50 ± 5% with food and water available ad libitum. Destabilization of the medial meniscus (DMM) was performed on the left knee joint of 8-week-old mice (n=8) without cutting the ligament as a control (n=8) and randomly divided into two groups for implantation of nanofiber. Eight weeks after DMM surgery, knee joint tissues were processed for histological analysis. All animal experiments were performed in accordance with the guidelines of the Institutional Animal Care and Use Committee (IACUC) of Wonkwang University and were approved by the Animal Ethics Committee of Wonkwang University (WKU21-05).

Histological Analysis

Cartilage samples were fixed with 10% neutral buffered formalin (NBF) for 24 h and decalcified using 0.5 M ethylenediaminetetraacetic acid (EDTA) solution for a week. After paraffin embedding, blocks were cut at 5 μM thickness and stained with safranin O. For immunohistochemical analysis, deparaffinized sections were incubated with primary antibodies overnight at 4 °C in a humidified chamber. Sections were developed using ImmPACT DAB (Vector Laboratories, #SK-4105). The following antibodies were used for immunohistochemical analysis: PPARγ (1:100 dilution, Abcam, #ab41928), IL-1β (1:100 dilution, Abcam, #ab9722), Bodipy (1:50 dilution, Thermo Fisher Scientific), and horseradish peroxidase (HRP)-conjugated goat anti-rabbit IgG (1:200 dilution, Enzo Life Sciences, #ADI-SAB-300).

Quantitative Real-Time Polymerase Chain Reaction (qRT-PCR)

qRT-PCR was performed using AMPIGENE qPCR Green Mix (Enzo Life Sciences, #ENZ-NUC104-1000). RN18S was used as an endogenous control. The qRT-PCR primer sequences used in this study are listed in Supplementary Table 1.

Results and Discussion

Preparation and Characterizations of CHI-GA/CK/PCL NFs

To prepare CK/PCL NFs with a one-sided coating of hydrophilic and adhesive materials, CHI-GA was synthesized by forming amide bond linkages. As shown in Figure 1a, the amine group of chitosan was reacted with the carboxylic acid group of gallic acid using EDC coupling agents. A peak at 265 nm was observed in the UV-Vis spectrum of CHI-GA due to the gallol groups (Figure 1b). In addition, the UV-Vis spectrum of CHI-GA was upshifted with a broad shoulder when CHI-GA was incubated for 8 h in phosphate-buffered saline (PBS) solution

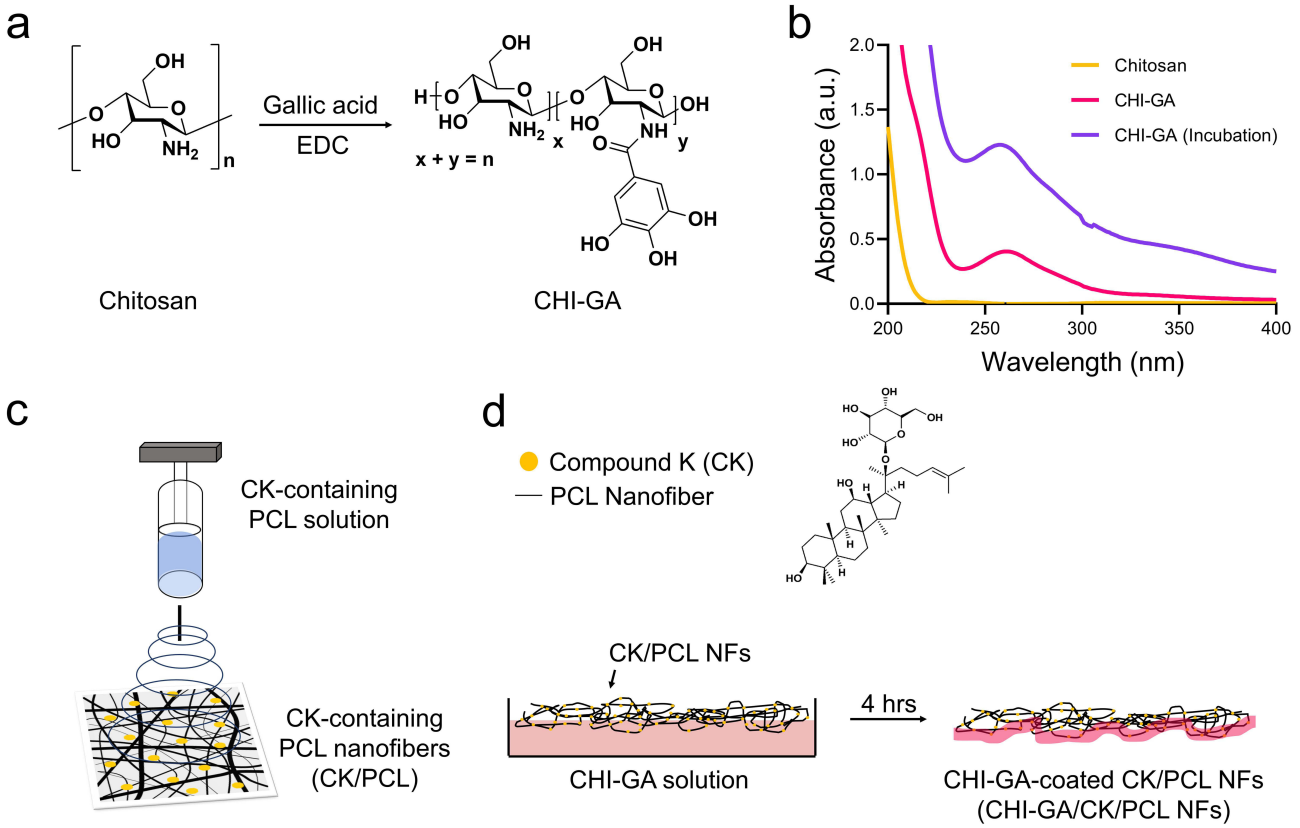

Figure 1 (**a**) Synthesis and chemical structures of CHI-GA. (**b**) UV-Vis spectra of chitosan, CHI-GA, and CHI-GA after incubation for 8 hrs. (**c** and **d**) Schematic illustrations of preparations of CK/PCL NFs (**c**) and CHI-GA-coated CK/PCL NFs (**d**).

(pH 7.4) due to the intra-and inter-molecular crosslinking of CHI-GA. As previously reported, the gallol moieties in the polymer backbones spontaneously are oxidized at neutral pH solutions.[53,54] In addition to hydrophilic and adhesive materials, CK/PCL NFs were prepared by electrospinning, as illustrated in Figure 1c. The CK/PCL NFs were then placed in the CHI-GA solution and incubated for 8 h. The CK/PCL NFs floated in the CHI-GA solution during the incubation because of the hydrophobicity of the PCL NFs (Figure 1d).

Figure 2 shows the morphological analysis of PCL (Figure 2a–d), CK/PCL (Figure 2e–h), and CHI-GA/CK/PCL NFs (Figure 2i–l) with the schematic illustrations. Scanning electron microscopy (SEM) images of PCL (Figure 2b and c), CK/PCL (Figure 2f and g), and CHI-GA/CK/PCL NFs (Figure 2j and k) were obtained to monitor the morphological changes after coating with CHI-GA. The average diameters obtained from the SEM images of CK/PCL NFs were 471.7 ± 244.4 nm, which were slightly smaller than that of the PCL NFs (602.2 ± 339.7 nm) (Figure 2d and h). Although there was no significance ($p > 0.5$) in diameters of NFs between two groups, the slight reduction in the diameter was probably due to the multiple hydroxyl groups of CK. As previously reported, the additives of small molecules that have multiple hydroxyl groups in the electrospinning of PCL affects the NF diameters by decreasing viscosity of solutions.[55,56] After the CHI-GA coating, the average diameters slightly increased to 563.1 ± 308.2 nm (Figure 2l). It also showed no significance ($p > 0.5$) in diameters of NFs between two groups, but the slight increase in the diameter was due to the formation of CHI-GA layers on CK/PCL NFs. Unexpectedly, several spots and/or defects in the CK/PCL NFs mesh were covered with CHI-GA polymers during the drying steps (Figure 2k). Vigorous washing steps using both PBS (pH 7.4) and distilled deionized water (DDW) after CHI-GA coatings of CK/PCL NFs could not prevent non-uniform coverage of PCL NFs with CHI-GA polymers. However, this was expected to increase the hydrophilic and adhesive properties on one side of the CK/PCL NFs.

Effects of Cell and Tissue Adhesiveness

The water contact angle (WCA) of the CHI-GA/CK/PCL NFs was monitored to confirm the enhanced hydrophilicity by CHI-GA coatings (Figure 3a and b). The WCA of CK/PCL NFs was 107.8 ± 5.8° similar to PCL NFs alone (111.4 ± 4.7°). After CHI-GA

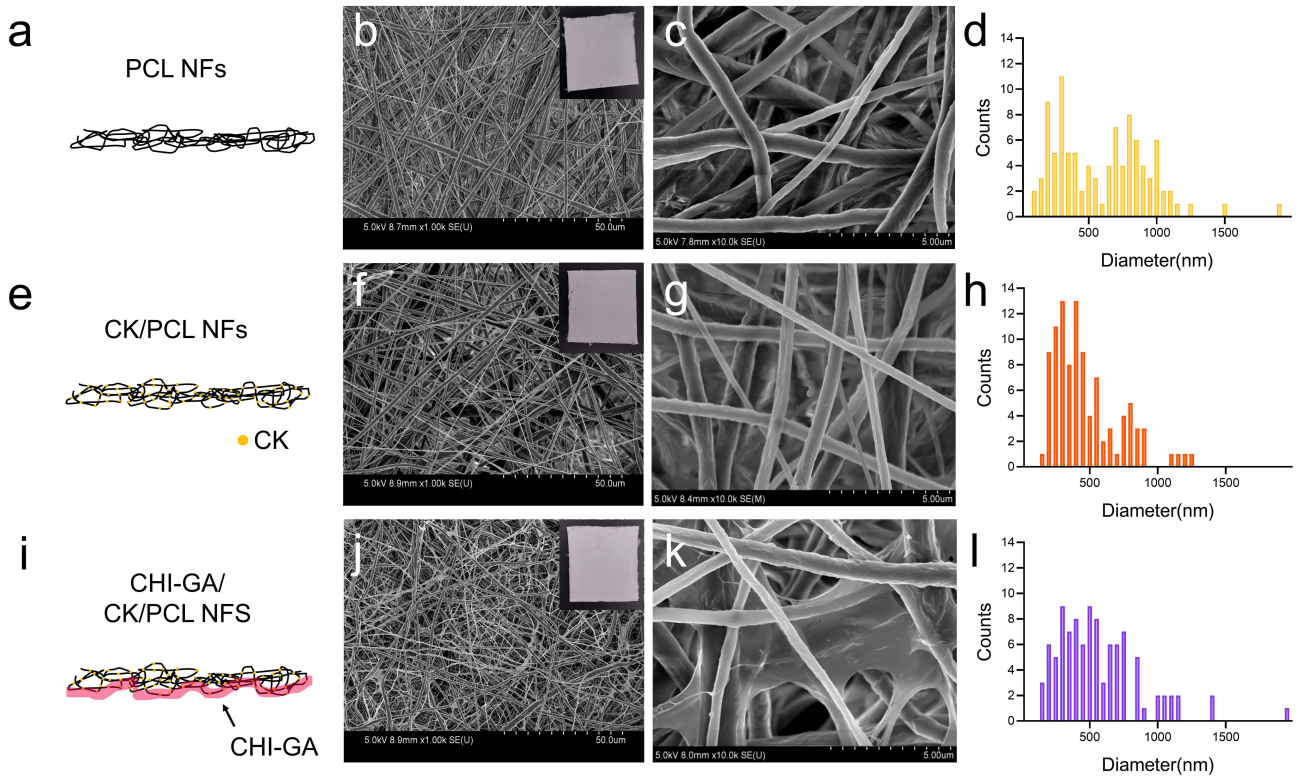

Figure 2 Morphological analysis of (**a–d**) PCL NFs, (**e–h**) CK/PCL NFs, and (**i–l**) CHI-GA/CK/PCL NFs. Schematic illustration (**a, e** and **i**), SEM images with 1 kX (**b, f** and **j**, scale bar: 50 μm) and 10 kX (**c, g** and **k** scale bar: 5 μm), and diameter distributions (**d, h** and **l**). The counts of NF diameters were measured with standard deviations of 100 NFs.

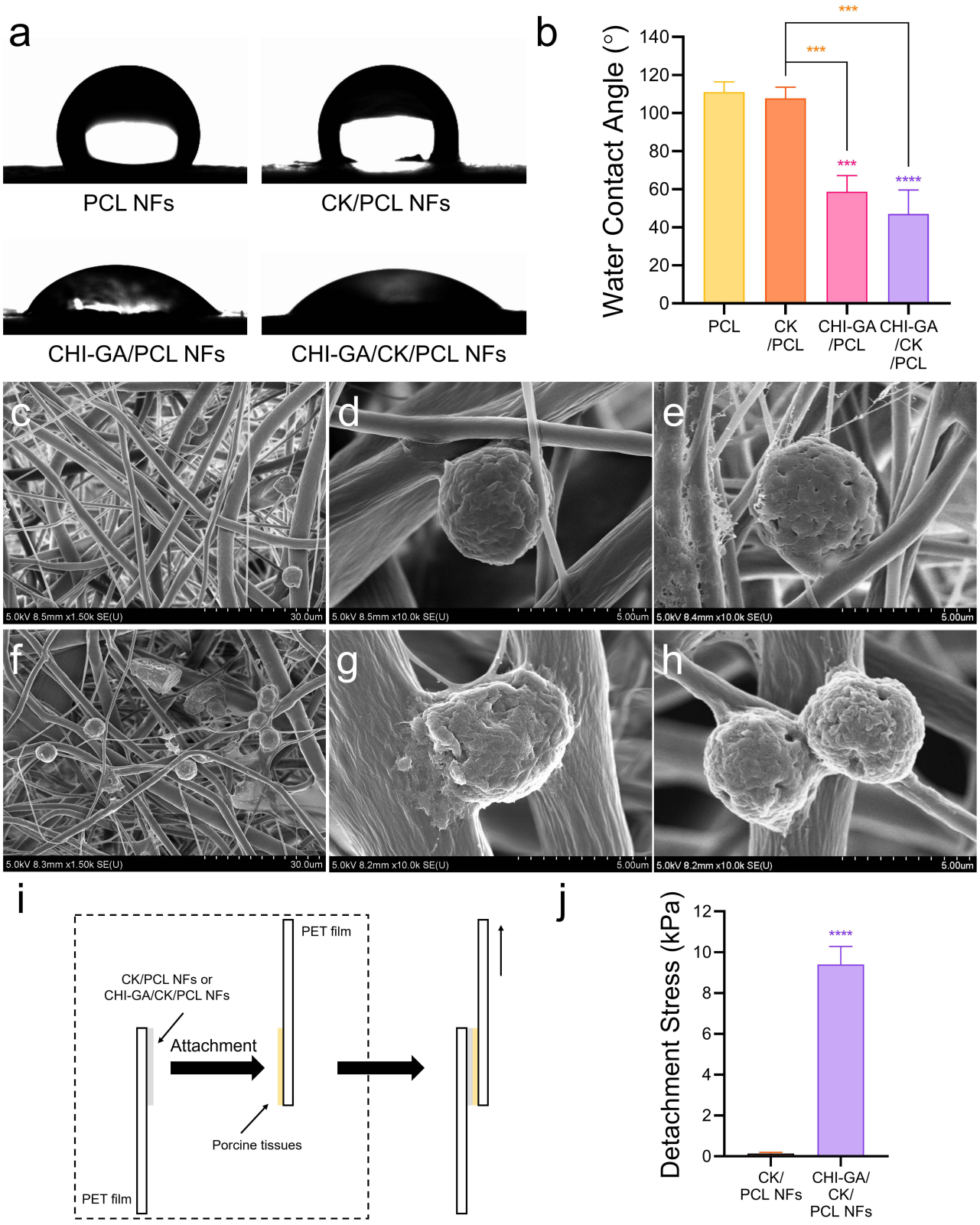

Figure 3 (**a**) Water contact angle (WCA) images and (**b**) average WCA of PCL, CK/PCL, CHI-GA/PCL, and CHI-GA/CK/PCL NFs. (**c–h**) SEM images of (**c–e**) CK/PCL NFs and (**f–h**) CHI-GA/CK/PCL NFs after cell attachment experiments with 1.5 kX (**c** and **f**, scale bar: 30 μm) and 10 kX (**d, e, g** and **h**, scale bar: 5 μm). (**i**) An illustration of tissue adhesion measurements. (**j**) Average detachment stress of CHI-GA/PCL and CHI-GA/CK/PCL NFs. ***P < 0.001, ****P < 0.0001.

coatings on the PCL and CK/PCL NFs, the WCAs were significantly decreased to 58.3 ± 8.7° and 47.5 ± 11.7° (P* < 0.01). The CHI-GA-coated CK/PCL NFs surfaces were hydrophilic, whereas the uncoated CK/PCL NFs surfaces were hydrophobic. Thus, the CHI-GA/CK/PCL NFs exhibited the opposite (ie, hydrophilic and hydrophobic) properties on the different sides. In addition, the adhesion of the cells and tissues to the CHI-GA/CK/PCL NFs was monitored. Cellular attachment to PCL NFs and cell morphology were evaluated using SEM. As shown in Figure 3c–h, the CHI-GA/CK/PCL NFs (Figure 3f–h) showed significantly increased cell density on the nanofibers compared with the unmodified CK/PCL NFs (Figure 3c–e). Moreover, the cells were strongly anchored to the CHI-GA/CK/PCL NFs with increased protrusion of the cell membranes. More importantly. Increased cellular and cell-to-cell contacts were observed in CHI-GA/CK/PCL NFs with elongated cells (Figure 3g and h). In PCL NFs, globular cells were more prominent (Figure 3d and e).

The tissue adhesion properties of the CHI-GA/CK/PCL NFs were measured using modified lap-shear test methods. As shown in Figure 3i, the PCL NFs side of the CHI-GA/CK/PCL NFs was attached to the adherend, and the porcine tissue was attached to another adherend. Then, the CHI-GA side of the CHI-GA/CK/PCL NFs and the porcine tissue were overlapped, and the tensile strengths were measured by pulling the film. As shown in Figure 3j, CHI-GA/CK/PCL NFs showed excellent tissue adhesiveness to porcine tissues (9.4 ± 0.7 kPa) compared with CK/PCL NFs (0.13 ± 0.05 kPa). Unexpectedly, the detachment stress of CK/PCL NFs increased 70-fold after coating with CHI-GA. This may be due to several defects in the CHI-GA polymer networks on the CK/PCL NFs meshes.

In vitro Assessments

To investigate the chondrogenic effects of CK on CHI-GA-coated nanofibers, immature mouse articular chondrocytes (iMACs) were isolated and cultured in PCL or CHI-GA-coated PCL with or without CK (Figure 4a). The anti-inflammatory effects of the nanofiber membranes were evaluated using real-time quantitative polymerase chain reaction (qRT-PCR). Catabolic biomarkers, including A disintegrin and metalloproteinase with thrombospondin motifs (ADAMTS)-4, −5, and matrix metalloproteinases (Mmp)-3, −5 or −13 were significantly inhibited by PCL and CHI/GA/PCL coated with CK (CK/PCL and CHI-GA/CK/PCL) compared to PCL or CHI-GA/PCL NFs, respectively (Figure 4b and c). The most dramatic reduction was observed in iMACs with CHI-GA/CK/PCL NFs. In addition, the expression levels of inflammatory markers, including C-C motif chemokine ligand (CCL)-4, −12, and interleukin-1β were significantly inhibited by the CK/PCL nanofibers compared to the PCL NFs (Figure 4d). The expression levels of CCL-2, −4, −5, CXC ligand-2, −3, and IL-1β were significantly inhibited by the CHI-GA/CK/PCL NFs compared to the CHI-GA/PCL NFs. Moreover, the CHI-GA/CK/PCL NFs showed the most significant decrease in the expression of these inflammation-related cytokines compared with the CK/PCL NFs. Recent studies have suggested that lipid accumulation is a key factor affecting the development and progression of OA, and the gene profiles involved in lipid metabolism have been examined.[57–59] Consistent with the expression profile of inflammatory biomarkers, a dramatic reduction in lipogenic genes was observed with CHI-GA/CK/PCL NFs compared to that with CHI-GA/PCL NFs. Moreover, the CHI-GA/CK/PCL NFs showed the highest decrease in the expression of lipogenic genes compared to the CK/PCL NFs.

Cartilage Regeneration Using CHI-GA/CK/PCL NFs

To investigate the therapeutic effects of the CHI-GA/CK/PCL NFs on the pathogenesis of OA, DMM was performed to induce OA pathological conditions (Figure 5a). Positive staining (red staining), indicating the secretion of glycosaminoglycans, a specific matrix for articular cartilage, significantly decreased in DMM-treated mice implanted with PCL or CHI-GA/PCL NFs (Figure 5b). The Osteoarthritis Research Society International (OARSI) score confirmed the progression of OA in DMM-induced mice implanted with PCL or CHI-GA/PCL NFs. However, the CHI-GA/CK/PCL NFs showed the most evident therapeutic effect on the alleviation of OA severity, with a decreased OARSI score compared to all other nanofibers (CHI-GA/PCL, CK/PCL, and PCL).

It has been suggested that the signaling mechanisms involved in lipid metabolism play an essential role in the pathogenesis of OA. Among these, peroxisome proliferator-activated receptor (PPAR) has been reported to be involved in reducing inflammatory responses in OA cartilage. Here, we found an increased level of PPARγ in DMM-induced cartilage implanted with CHI-GA/PCL and CHI-GA/CK/PCL NFs (Figure 5c). However, the expression level of PPARγ did not change with the implantation of PCL or CK/PCL NFs. Previously, it was reported that the deficiency of PPARγ

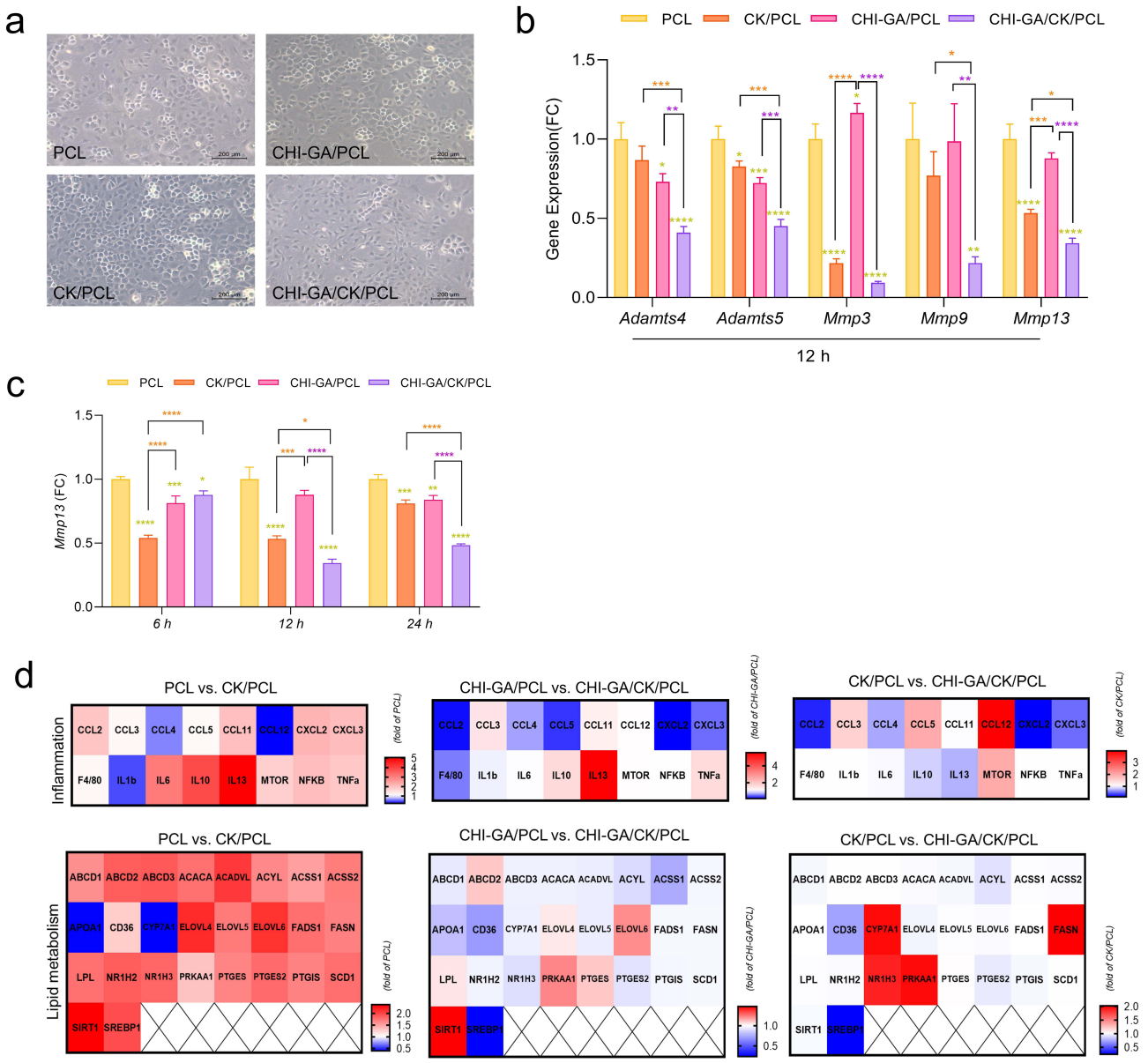

Figure 4 (**a**) Optical images of cells in PCL, CK/PCL, CHI-GA/PCL, and CHI-GA/CK/PCL NFs. (**b**) Expression level of cartilage degrading genes. (**c**) Expression level of the Mmp13 gene. (**d**) Expression level of genes involved in inflammation and lipid metabolism. *P < 0.05; **P < 0.01; ***P < 0.001, ****P < 0.0001.

increases the catabolic activity of MMPs and inflammatory factors such as IL-1β, IL-6, and tumor necrosis factor-α in the articular cartilage and contributes to cartilage destruction and the progression of OA.[59] Consistent with this, lipid accumulation (Figure 6a) and the expression level of IL-1β (Figure 6b) were also significantly reduced by the implantation of CHI-GA/PCL and CHI-GA/CK/PCL NFs in DMM-induced cartilage. To see whether gallic acid-conjugation affects the cellular adhesion, iMACs were cultures with BSA, CHI, or CHI-GA coated glass surface. Notably, the CHI-GA-coated glass surface exhibited the highest cell adhesion properties (Figure 7a). Furthermore, cytoskeleton staining also indicated a strong intensity in cells cultured on CHI-GA coated glass surface (Figure 7b). Gallol-containing molecules can enhance the cell adhesion with functionalities such as anti-inflammatory and anti-oxidative properties, as previous reported.[60] It was noteworthy that gallol groups of CHI-GA significantly enhanced the cell attachments on the substrates that could provide the therapeutic strategy for cartilage regenerations.

To validate the enhanced cellular effects of CHI-GA/CK/PCL NFs, iMACs were treated with CK, CHI, or CK/CHI-CA. Since cell adhesion is accomplished by the cell adhesion molecules located on the cell surface such as integrins,[61]

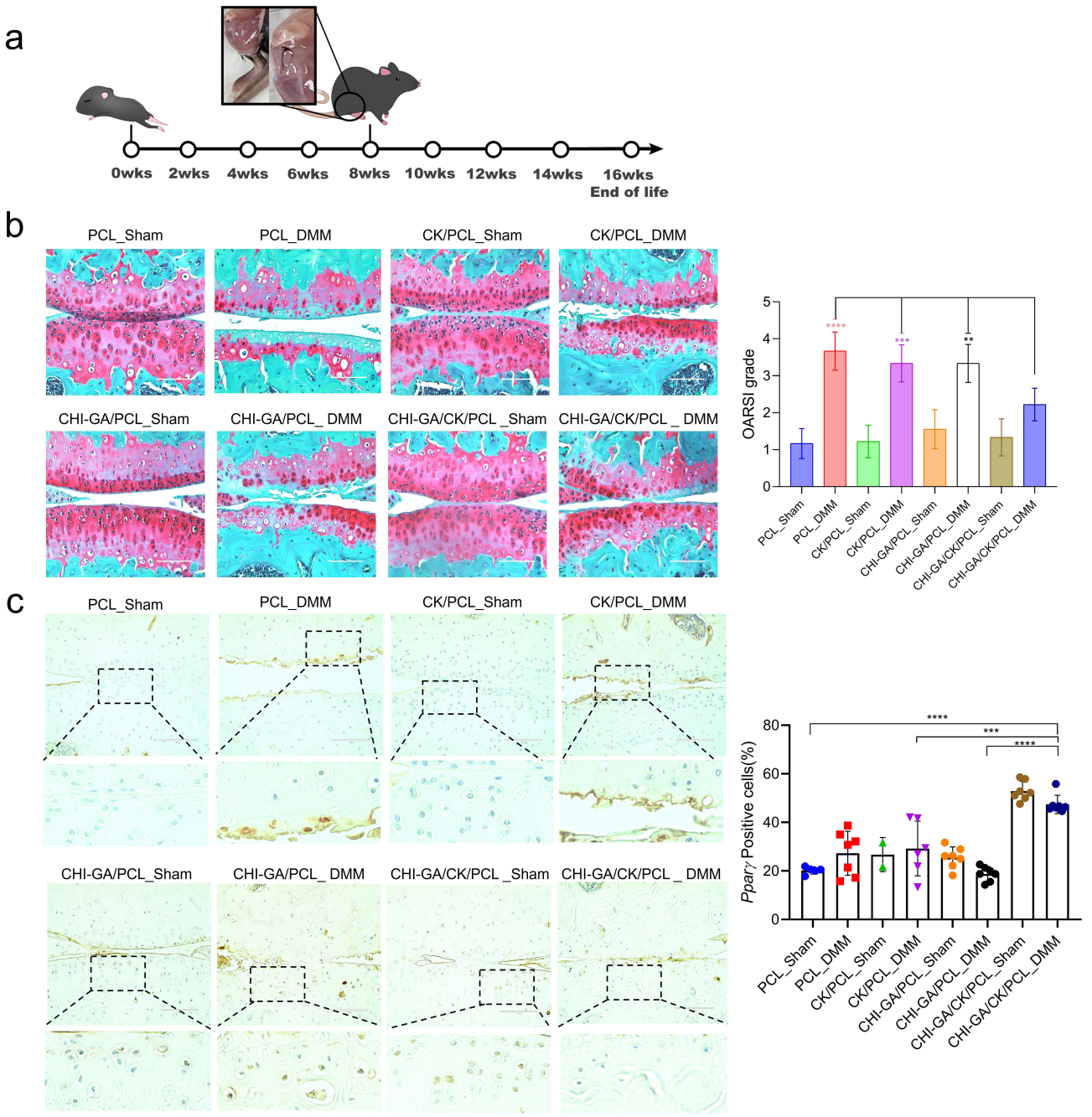

Figure 5 (**a**) Experimental scheme. (**b**) Safranin O staining and OARSI score. (**c**) Immunohistochemistry of PPARγ (left panel) and percentage of PPARγ-positive cells (right panel). **P < 0.01; ***P < 0.001, ****P < 0.0001, Scale bar: 100 μm.

the expression level of integrins were analyzed. Exposure to CK/CHI-GA significantly increased the expression level of *ITGα1, ITGα5, ITGα10*, and *ITGα1* compared to CK or CHI treatment (Figure 7c). Additionally, an increased level of *pparα* and *pparγ* recognized as promising therapeutic targets for the prevention of OA progression,[62,63] was observed with CK/CHI-GA treatment (Figure 7d). Our findings indicate that CHI-GA/PCL demonstrates a therapeutic effect in osteoarthritis (OA) pathogenesis by improving chondrocyte adhesion and preventing cartilage degradation through the upregulation of integrin levels and stimulation of the PPARγ pathway. While the DMM model in mice is widely acknowledged for its high reproducibility and its ability to induce moderate to severe cartilage lesions,[64] it's crucial to understand the inherent differences between mice and humans. Due to their considerably smaller size compared to

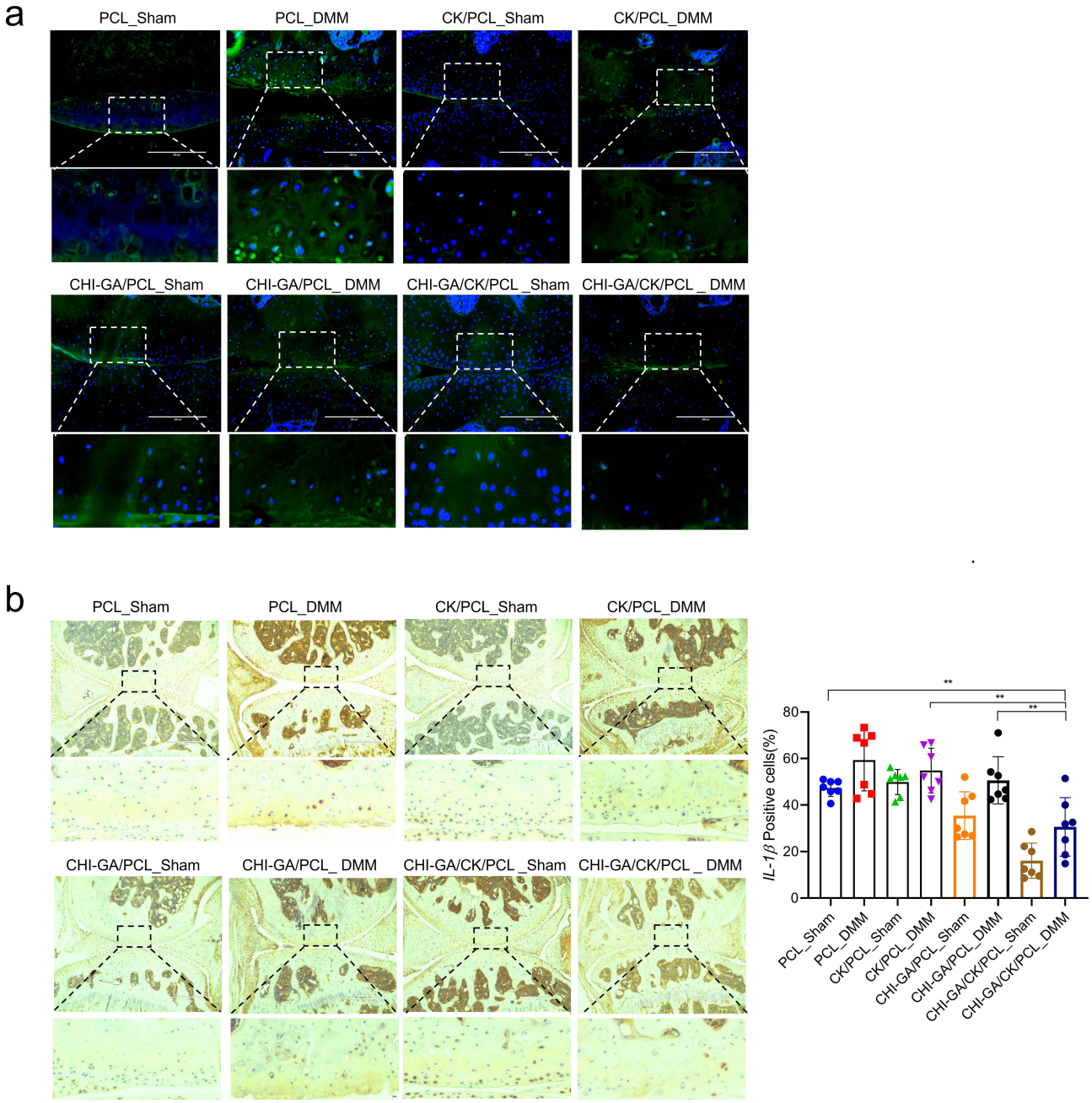

Figure 6 (**a**) Bodipy staining. Scale bar: 200 μm. (**b**) Immunohistochemistry of IL-1β (left panel) and percentage of IL-1β positive cells (right panel). Scale bar: 400 μm. **P < 0.01.

human, mice undergo substantial biomechanical stress on their joints, a factor that should not be overlooked or underestimated. Moreover, there are notable anatomical differences in mouse cartilage, such as differences in overall thickness, the presence of a thick layer of calcified cartilage, and the absence of distinct superficial, transitional, and radial zones of chondrocytes. In addition, recent reports have highlighted the impact of the interplay between muscle or bone on cartilage degeneration.[65,66] Hence, it may be important to explore the potential correlation between the inhibitory effects of CHI-GA/CK/PCL NFs on cartilage degeneration and their interaction with muscle or bone might be crucial and related research is currently ongoing.

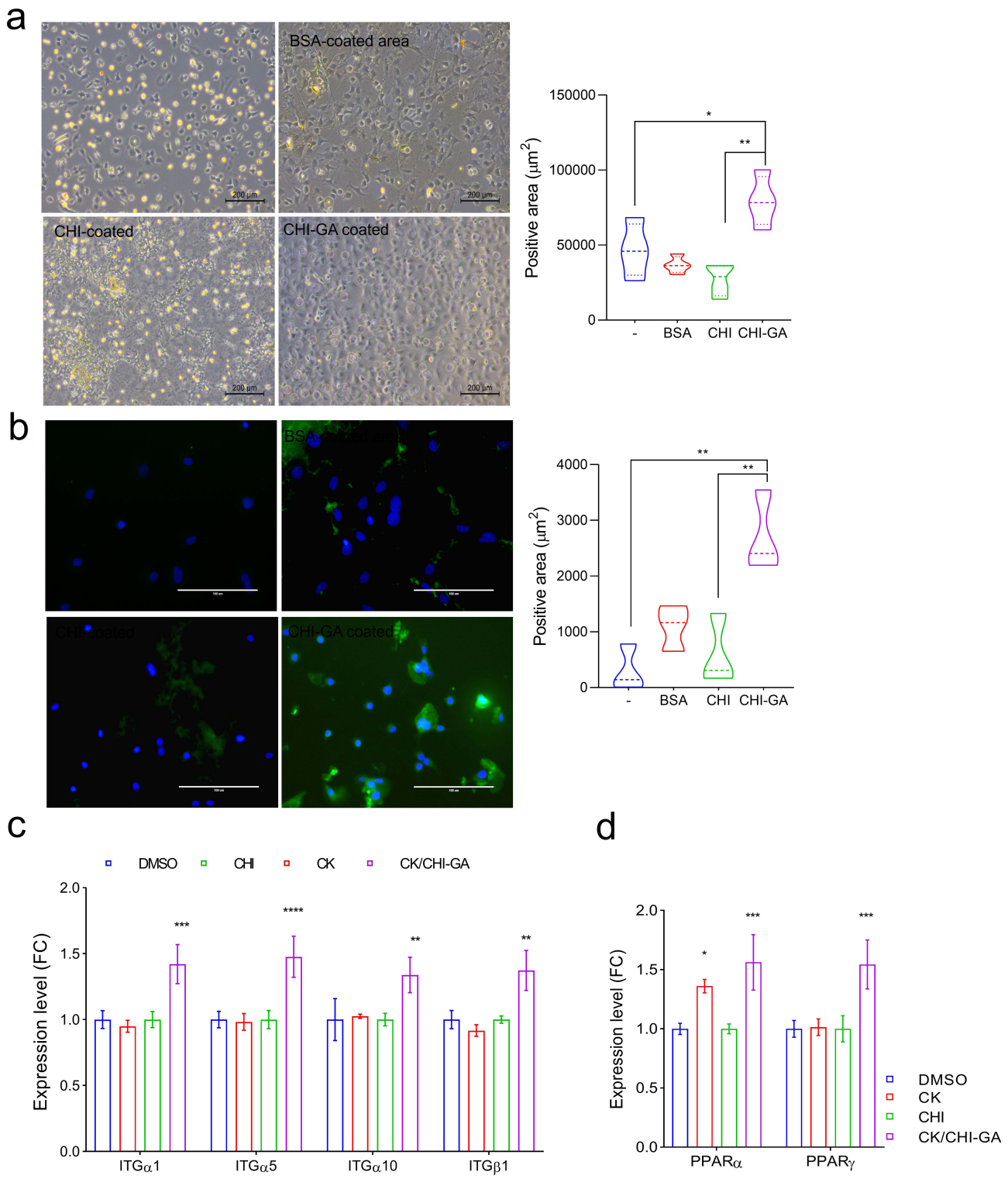

Figure 7 (**a**) Bright field image. (**b**) Immunohistochemistry of phalloidin staining. The positive area for adherent cells and phalloidin staining was measured by Image Pro software. (**c**) Expression level of integrin genes. Measured by Image Pro software. (**d**) Expression level of PPARα and PPARγ genes. *P < 0.05; **P < 0.01; ***P < 0.001, ****P < 0.0001.

Conclusion

In summary, hydrophilic and adhesive CHI-GA-coated compound K-loaded PCL NFs were developed for cartilage tissue regeneration. The CHI-GA-coated surfaces of the CK/PCL NFs exhibited excellent cell (ie, increased up to 50%) and tissue adhesive properties with hydrophilicity. Furthermore, the CHI-GA layer within the CK/PCL NFs demonstrated an

increased adhesion to cartilage defects and CK demonstrated a significant therapeutic efficacy in cartilage regeneration, exhibiting a remarkable improvement of up to 60% according to OARSI scoring. CHI-GA/CK/PCL increased the expression level of integrins up to 20% compared to CK-treated chondrocytes, decreased the major cartilage-degrading enzyme MMP13, up to 60% compared to OA chondrocytes and inflammatory cytokine, IL-1β up to 50% compared to PCL-DMM cartilage possibly through increased peroxisome proliferator-activated receptor (PPAR). Our study proved that these CK-loaded hydrophilic adhesive nanofibers and simple coating methods have an enormous potential in cartilage tissue regeneration.

Abbreviations

PCL, polycaprolactone; NFs, nanofibers; CHI-GA, gallic acid-conjugated chitosan; CK, compound K; DMM, destabilization of the medial meniscus; IL-1β, interleukin-1β; PPAR, peroxisome proliferator-activated receptor; OA, osteoarthritis; MMPs, matrix metalloproteinases; NMR, nuclear magnetic resonance; UV-Vis, ultraviolet-visible; SEM, scanning electron microscope, WCA, water contact angle; ADAMTS, A disintegrin and metalloproteinase with thrombospondin motifs; OARSI, Osteoarthritis Research Society International.

Acknowledgments

This work was supported by the National Research Foundation of Korea (NRF) grant funded by the Korea Government (MSIT) (2022R1A4A1031259 and 2021R1I1A3041149) to E-JJ. and supported by the Korean Fund for Regenerative Medicine (KFRM) grant funded by the Korea government (the Ministry of Science and ICT, the Ministry of Health & Welfare) (22A0103L1) to JHR.

Disclosure

Professor Ji Hyun Ryu reports a patent DRUG DELIVERY SYSTEM AND ITS MACUFACTURING METHOD pending to Wonkwang University (Yeo Jin Kim, Dong Hyeon Kim, June Young Park, Ji Hyun Ryu, Eun-Jung Jin). The authors report no other conflicts of interest in this work.

References

1. Bhosale AM, Richardson JB. Articular cartilage: structure, injuries and review of management. *Br Med Bull*. 2008;87(1):77–95. doi:10.1093/bmb/ldn025
2. Bedi A, Feeley BT, Williams RJ. Management of articular cartilage defects of the knee. *J Bone Jt Surg*. 2010;92(4):994–1009. doi:10.2106/JBJS.I.00895
3. Wieland HA, Michaelis M, Kirschbaum BJ, et al. Osteoarthritis-an untreatable disease? *Nat Rev Drug Discov*. 2005;4(4):331–344. doi:10.1038/nrd1693
4. Armiento AR, Stoddart MJ, Alini M, et al. Biomaterials for articular cartilage tissue engineering: learning from biology. *Acta Biomater*. 2018;65:1–20. doi:10.1016/j.actbio.2017.11.021
5. Makris EA, Gomoll AH, Malizos KN, et al. Repair and tissue engineering techniques for articular cartilage. *Nat Rev Rheumatol*. 2015;11(1):21–34. doi:10.1038/nrrheum.2014.157
6. Rana D, Ratheesh G, Ramakrishna S, et al. *Ch 13. Nanofiber Composites in Cartilage Tissue Engineering, Nanofiber Composite for Biomedical Applications*. Woodhead Publishing; 2017:325–344.
7. Chen W, Chen S, Morsi Y, et al. Superabsorbent 3D scaffold based on electrospun nanofibers for cartilage tissue engineering. *ACS Appl Mater Interfaces*. 2016;8(37):24415–24425. doi:10.1021/acsami.6b06825
8. Li WJ, Jiang YJ, Tuan RS. Cell-nanofiber-based cartilage tissue engineering using improved cell seeding, growth factor, and bioreactor technologies. *Tissue Eng Part A*. 2018;14(5):639–648. doi:10.1089/tea.2007.0136
9. Chen W, Xu Y, Liu Y, et al. Three-dimensional printed electrospun fiber-based scaffold for cartilage regeneration. *Mater Des*. 2019;179:107886. doi:10.1016/j.matdes.2019.107886
10. Raja IS, Lee SH, Kang MS, et al. The predominant factor influencing cellular behavior on electrospun nanofibrous scaffolds: wettability or surface morphology? *Mater Des*. 2022;216:110580. doi:10.1016/j.matdes.2022.110580
11. Ahmadian E, Eftekhari A, Janas D, et al. Nanofiber scaffolds based on extracellular matrix for articular cartilage engineering: a perspective. *Nanotheranostics*. 2023;7(1):61–69. doi:10.7150/ntno.78611
12. Wade RJ, Burdick JA. Advances in nanofibrous scaffolds for biomedical applications: from electrospinning to self-assembly. *Nano Today*. 2014;9(6):722–742. doi:10.1016/j.nantod.2014.10.002
13. Vasita R, Katti DS. Nanofibers and their applications in tissue engineering. *Int J Nanomed*. 2006;1(1):15–30. doi:10.2147/nano.2006.1.1.15
14. Son HY, Ryu JH, Lee H, et al. Silver-polydopamine hybrid coatings of electrospun poly(vinyl alcohol) nanofibers. *Macromol Mater Eng*. 2013;298(5):547–554. doi:10.1002/mame.201200231

15. Venugopal J, Low S, Choon AT, et al. Interaction of cells and nanofiber scaffolds in tissue engineering. *J Biomed Mater Res B*. 2008;84(1):34–48. doi:10.1002/jbm.b.30841
16. Chen JP, Su CH. Surface modification of electrospun PLLA nanofibers by plasma treatment and cationized gelatin immobilization for cartilage tissue engineering. *Acta Biomater*. 2011;7(1):234–243. doi:10.1016/j.actbio.2010.08.015
17. Lu Y, Huang J, Yu G, et al. Coaxial electrospun fibers: applications in drug delivery and tissue engineering. *Wiley Interdiscip Rev Nanomed Nanobiotechnol*. 2016;8(5):654–677. doi:10.1002/wnan.1391
18. Buzgo M, Jakubova R, Mickova A, et al. Time-regulated drug delivery system based on coaxially incorporated platelet α-granules for biomedical use. *Nanomedicine*. 2013;8(7):1137–1154. doi:10.2217/nnm.12.140
19. Mondal D, Griffith M, Venkatraman SS. Polycaprolactone-based biomaterials for tissue engineering and drug delivery: current scenario and challenges. *Int J Polym Mater Polym Biomater*. 2016;65(5):255–265. doi:10.1080/00914037.2015.1103241
20. Suwantong O. Biomedical applications of electrospun polycaprolactone fiber mats. *Polym Adv Technol*. 2016;27(10):1264–1273. doi:10.1002/pat.3876
21. Janmohammadi M, Nourbakhsh MS. Electrospun polycaprolactone scaffolds for tissue engineering: a review. *Int J Polym Mater Polym Biomater*. 2019;68(9):527–539. doi:10.1080/00914037.2018.1466139
22. Girao AF, Semitela A, Ramalho G, et al. Mimicking nature: fabrication of 3D anisotropic electrospun polycaprolactone scaffolds for cartilage tissue engineering applications. *Comp B Eng*. 2018;154:99–107. doi:10.1016/j.compositesb.2018.08.001
23. Son HY, Ryu JH, Lee H, et al. Bioinspired templating synthesis of metal–polymer hybrid nanostructures within 3D electrospun nanofibers. *ACS Appl Mater Interfaces*. 2013;5(13):6381–6390. doi:10.1021/am401550p
24. Gupta N, Rao SK, Jaison D, et al. Kaempferol loaded albumin nanoparticles and dexamethasone encapsulation into electrospun polycaprolactone fibrous mat-concurrent release for cartilage regeneration. *J Drug Deliv Sci Technol*. 2021;64:102666. doi:10.1016/j.jddst.2021.102666
25. Asadian M, Onyshchenko I, Thiry D, et al. Thiolation of polycaprolactone (PCL) nanofibers by inductively coupled plasma (ICP) polymerization: physical, chemical and biological properties. *Appl Surf Sci*. 2019;479:942–952. doi:10.1016/j.apsusc.2019.02.178
26. Zhang YZ, Venugopal J, Huang ZM, et al. Characterization of the surface biocompatibility of the electrospun PCL-collagen nanofibers using fibroblasts. *Biomacromolecules*. 2005;6(5):2583–2589. doi:10.1021/bm050314k
27. Yaseri R, Fadaie M, Mirzaei E, et al. Ebrahiminezhad, Surface modification of polycaprolactone nanofibers through hydrolysis and aminolysis: a comparative study on structural characteristics, mechanical properties, and cellular performance, Sci. *Rep*. 2023;13(1):9434.
28. Lo HY, Kuo HT, Huang YY. Application of polycaprolactone as an anti-adhesion biomaterial film. *Artif Organs*. 2010;34(8):648–653. doi:10.1111/j.1525-1594.2009.00949.x
29. Chen CH, Chen SH, Shalumon KT, et al. Prevention of peritendinous adhesions with electrospun polyethylene glycol/polycaprolactone nanofibrous membranes. *Colloids Surf B*. 2015;133:221–230. doi:10.1016/j.colsurfb.2015.06.012
30. Martins A, Pinho ED, Faria S, et al. Surface modification of electrospun polycaprolactone nanofiber meshes by plasma treatment to enhance biological performance. *Small*. 2009;5(10):1195–1206. doi:10.1002/smll.200801648
31. Yew CHT, Azari P, Choi JR, et al. Electrospun polycaprolactone nanofibers as a reaction membrane for lateral flow assay. *Polymers*. 2018;10(12):1387. doi:10.3390/polym10121387
32. Rashtchian M, Hivechi A, Bahrami SH, et al. Fabricating alginate/poly (caprolactone) nanofibers with enhanced bio-mechanical properties via cellulose nanocrystal incorporation. *Carbohydr Polym*. 2020;233:115873. doi:10.1016/j.carbpol.2020.115873
33. Liu Y, Tian K, Hao J, et al. Biomimetic poly(glycerol sebacate)/polycaprolactone blend scaffolds for cartilage tissue engineering. *J Mater Sci Mater Med*. 2019;30(5):53. doi:10.1007/s10856-019-6257-3
34. Sharifi F, Irani S, Azadegan G, et al. Co-electrospun gelatin-chondroitin sulfate/polycaprolactone nanofibrous scaffolds for cartilage tissue engineering. *Bioact Carbohydr Diet Fibre*. 2020;22:100215. doi:10.1016/j.bcdf.2020.100215
35. Shirehjini LM, Sharifi F, Shojaei S, et al. Poly-caprolactone nanofibrous coated with sol-gel alginate/mesenchymal stem cells for cartilage tissue engineering. *J Drug Deliv Sci and Technol*. 2022;74:103488. doi:10.1016/j.jddst.2022.103488
36. Piai JF, da Silva MA, Martins A, et al. Chondroitin sulfate immobilization at the surface of electrospun nanofiber meshes for cartilage tissue regeneration approaches. *Appl Surf Sci*. 2017;403:112–125. doi:10.1016/j.apsusc.2016.12.135
37. Lee P, Tran K, Chang W, et al. Influence of chondroitin sulfate and hyaluronic acid presence in nanofibers and its alignment on the bone marrow stromal cells: cartilage regeneration. *J Biomed Nanotechnol*. 2014;10(8):1469–1479. doi:10.1166/jbn.2014.1831
38. Kabirkoohian A, Bakhshi H, Irani S, et al. Chemical immobilization of carboxymethyl chitosan on polycaprolactone nanofibers as osteochondral scaffolds. *Appl Biochem Biotechnol*. 2023;195(6):3888–3899. doi:10.1007/s12010-022-03916-6
39. Yang XD, Yang YY, Ouyang DS, et al. A review of biotransformation and pharmacology of ginsenoside compound K. *Fitoterapia*. 2015;100:208–220. doi:10.1016/j.fitote.2014.11.019
40. Liu T, Zhu L, Wang L. A narrative review of the pharmacology of ginsenoside compound K. *Ann Transl Med*. 2022;10(4):234. doi:10.21037/atm-22-501
41. Yang JH, Shin HH, Kim D, et al. Adhesive ginsenoside compound K patches for cartilage tissue regeneration. *Regen Biomater*. 2023;10:rbad077.
42. Sophia Fox AJ, Bedi A, Rodeo SA. The basic science of articular cartilage: structure, composition, and function. *Sports Health*. 2009;1(6):461–468. doi:10.1177/1941738109350438
43. Park D, Yoon M. Compound K, a novel ginsenoside metabolite, inhibits adipocyte differentiation in 3T3-L1 cells: involvement of angiogenesis and MMPs. *Biochem Biophys Res Commun*. 2012;422(2):263–267. doi:10.1016/j.bbrc.2012.04.142
44. Ryu JH, Messersmith PB, Lee H. Polydopamine surface chemistry: a decade of discovery. *ACS Appl Mater Interfaces*. 2018;10(9):7523–7540. doi:10.1021/acsami.7b19865
45. Choi SM, Jung HW, Ryu JH, et al. Effect of polydopamine and fluoride ion coating on dental enamel remineralization: an in vitro study. *BMC Oral Health*. 2023;23(1):526. doi:10.1186/s12903-023-03221-6
46. Kim S, Gim T, Jeong Y, et al. Facile construction of robust multilayered PEG films on polydopamine-coated solid substrates for marine antifouling applications. *ACS Appl Mater Interfaces*. 2017;10(9):7626–7631. doi:10.1021/acsami.7b07199
47. Nasibova A. Generation of nanoparticles in biological systems and their application prospects. *Adv Biol Earth Sci*. 2023;8(2):140–146.
48. Ramazanli VN. Effect of pH and temperature on the synthesis of silver nanoparticles extracted from olive leaf. *Adv Biol Earth Sci*. 2021;6(2):169–173.

49. Ahmadov IS, Bandaliyeva AA, Nasibova AN, et al. The synthesis of the silver nanodrugs in the medicinal plant Baikal skullcap (Scutellaria baicalensis Georgi) and their antioxidant, antibacterial activity. *Adv Biol Earth Sci*. 2020;5(2):103–118.
50. Kang SI, Shin HH, Yoon G, et al. Double-layer adhesives for preventing anastomotic leakage and reducing post-surgical adhesion. *Mater Today Bio*. 2023;23:100806. doi:10.1016/j.mtbio.2023.100806
51. Shin HH, Ryu JH. Bio-inspired self-healing, shear-thinning, and adhesive gallic acid-conjugated chitosan/carbon black composite hydrogels as suture support materials. *Biomimetics*. 2023;8(7):54. doi:10.3390/biomimetics8070542
52. Kwon HJ, Shin HH, Hyun DH, et al. Carbon black-containing self-healing adhesive hydrogels for endoscopic tattooing. *Sci Rep*. 2023;13(1):1880. doi:10.1038/s41598-023-28113-1
53. Ju J, Jin S, Kim S, et al. Addressing the shortcomings of polyphenol-derived adhesives: achievement of long shelf life for effective hemostasis. *ACS Appl Mater Interfaces*. 2022;14(22):25115–25125. doi:10.1021/acsami.2c03930
54. Sanandiya ND, Lee S, Rho S, et al. Tunichrome-inspired pyrogallol functionalized chitosan for tissue adhesion and hemostasis. *Carbohydr Polym*. 2019;208:77–85. doi:10.1016/j.carbpol.2018.12.017
55. Zeng W, Cheng N-M, Liang X, et al. Electrospun polycaprolactone nanofibrous membranes loaded with baicalin for antibacterial wound dressing. *Sci Rep*. 2022;12(1):10900. doi:10.1038/s41598-022-13141-0
56. Wang D, Jang J, Kim K, et al. "Tree to bone": lignin/polycaprolactone nanofibers for hydroxyapatite biomineralization. *Biomacromolecules*. 2019;20(7):2684–2693. doi:10.1021/acs.biomac.9b00451
57. Song J, Baek IJ, Chun CH, et al. Dysregulation of the NUDT7-PGAM1 axis is responsible for chondrocyte death during osteoarthritis pathogenesis. *Nat Commun*. 2018;9(1):3427. doi:10.1038/s41467-018-05787-0
58. Park S, Oh J, Kim YI, et al. Suppression of ABCD2 dysregulates lipid metabolism via dysregulation of miR-141:ACSL4 in human osteoarthritis. *Cell Biochem Funct*. 2018;36(7):366–376. doi:10.1002/cbf.3356
59. Park S, Baek IJ, Ryu JH, et al. PPARα− ACOT12 axis is responsible for maintaining cartilage homeostasis through modulating de novo lipogenesis. *Nat Commun*. 2022;13(1):3. doi:10.1038/s41467-021-27738-y
60. Chen Y, Xu W, Shafiq M, et al. Injectable nanofiber microspheres modified with metal phenolic networks for effective osteoarthritis treatment. *Acta Biomater*. 2023;157:593–608. doi:10.1016/j.actbio.2022.11.040
61. Morgan M, Humphries M, Bass M. Synergistic control of cell adhesion by integrins and syndecans. *Nat Rev Mol Cell Biol*. 2007;8(12):957–969. doi:10.1038/nrm2289
62. Stienstra R, Mandard S, Patsouris D, et al. Peroxisome proliferator-activated receptor alpha protects against obesity-induced hepatic inflammation. *Endocrinology*. 2007;148:2753–2763.
63. Zhou JL, Liu SQ, Qiu B, et al. The protective effect of sodium hyaluronate on the cartilage of rabbit osteoarthritis by inhibiting peroxisome proliferator-activated receptor gamma messenger RNA expression. *Yonsei Med J*. 2009;50(6):832–837. doi:10.3349/ymj.2009.50.6.832
64. Culley KL, Dragomir CL, Chang J, et al. Mouse models of osteoarthritis: surgical model of posttraumatic osteoarthritis induced by destabilization of the medial meniscus. *Methods Mol Biol*. 2015;1226:143–173.
65. Ciliberti FK, Aubonnet R, Ramos J, et al. Novel strategies for cartilage assessment, interplay between bone and muscles. *Eur J Transl Myol*. 2023;33:67–68.
66. Lin C, Liu L, Zeng C, et al. Activation of mTORC1 in subchondral bone preosteoblasts promotes osteoarthritis by stimulating bone sclerosis and secretion of CXCL12. *Bone Res*. 2019;7(1):5. doi:10.1038/s41413-018-0041-8